JBC Papers in Press. Published on June 21, 2017 as Manuscript M117.778654
The latest version is at http://www.jbc.org/cgi/doi/10.1074/jbc.M117.778654

Hydrogen sulfide modulates eukaryotic translation initiation factor 2α (eIF2α) phosphorylation status in the integrated stress response pathway

Vinita Yadav[1], Xing-Huang Gao[2], Belinda Willard[3], Maria Hatzoglou[2], Ruma Banerjee[1], Omer Kabil[1]*

[1]Department of Biological Chemistry, University of Michigan Medical School, Ann Arbor, MI. [2]Department of Genetics and Genome Sciences, Case Western Reserve University, Cleveland, OH. [3]Proteomics and Metabolomics Laboratory, Lerner Research Institute, Cleveland Clinic, Cleveland, OH.

Running title: Regulation of integrated stress response pathway by H_2S

*To whom correspondence should be addressed. E-mail: omerk@umich.edu

Keywords: Hydrogen sulfide, integrated stress response, cytoprotection, protein persulfidation, sulfhydration, PP1c

ABSTRACT

Hydrogen sulfide (H_2S) regulates various physiological processes including neuronal activity, vascular tone, inflammation, and energy metabolism. Moreover, H_2S elicits cytoprotective effects against stressors in various cellular models of injury. However, the mechanism of the signaling pathways mediating the cytoprotective functions of H_2S is not well understood. We previously uncovered a heme-dependent metabolic switch for transient induction of H_2S production in the transsulfuration pathway. Here, we demonstrate that increased endogenous H_2S production or its exogenous administration modulates major components of the integrated stress response (ISR) promoting a metabolic state primed for stress response. We show that H_2S transiently increases phosphorylation of eukaryotic translation initiation factor 2 (eIF2α) resulting in inhibition of general protein synthesis. The H_2S-induced increase in eIF2α phosphorylation (eIF2α-P) was mediated at least in part by inhibition of protein phosphatase-1 (PP1c) via persulfidation at Cys127. Overexpression of a PP1c cysteine mutant (C127S-PP1c) abrogated the H_2S effect on eIF2α phosphorylation. Our data supports a model in which H_2S exerts its cytoprotective effect on ISR signaling by inducing a transient adaptive reprogramming of global mRNA translation. While a transient increase in endogenous H_2S production provides cytoprotection, its chronic increase such as in CBS deficiency may pose a problem.

INTRODUCTION

Cells respond to endogenously produced and external stressors that perturb cellular homeostasis by activating stress response pathways to adapt to stressful conditions and to minimize damage to cellular components. Recent findings have uncovered a significant regulatory role for H_2S signaling on this front and fueled a growing pharmacological interest in H_2S for treatment of cardiovascular diseases and inflammation where stress-induced cell injury contributes significantly to disease progression (1,2). H_2S is a signaling molecule produced endogenously from sulfur containing amino acids, cysteine and homocysteine, by the actions of two enzymes in the transsulfuration pathway, cystathionine β-synthase (CBS) and cystathionine γ-lyase (CSE) (3), and from 3-mercaptopyruvate catalyzed by mercaptopyruvate sulfur transferase (4,5). Metabolic removal of H_2S involves its oxidation in mitochondria to

thiosulfate and sulfate (6), which are excreted in urine (7). H_2S is a weak acid and ionizes to HS^- and H^+ with a pKa of 6.9 (8) resulting in an estimated 80% of it being in the ionized form at physiological pH. While HS^- is likely confined to cells in which it is produced, H_2S gas can freely diffuse across membranes (9) to initiate paracrine signaling i.e., at sites remote from its production site. H_2S–based signaling is mediated by formation of persulfides at reactive cysteine residues on target proteins to change activity (10). Persulfides can form via reaction of HS^- with oxidized cysteine on proteins such as cysteine sulfenic acid, or by the reaction of cysteine thiolates on oxidized sulfide species such as HSSH and polysulfides (11).

Besides regulating vascular tone (12-18) and neuronal activity (3,19), H_2S provides profound cytoprotective effects. H_2S treatment reduces oxidative injury during ischemia-reperfusion in various organ systems (20-22) and protects from heart failure in disease models (23-26). It protects neuronal cells from oxidative stress (27-31), and from the cytotoxic effect of β-amyloid peptides (32,33). H_2S treatment also increases resistance to ER stress in neuronal cells (34,35), cardiomyocytes (36) and endothelial cells (37). It suppresses ER-induced endothelial to mesenchymal transdifferentiation (37), a pathologic factor for progression of cardiac fibrosis (38) and reprograms cellular energy production in pancreatic beta cells in response to chronic ER stress (39). While the mechanism of H_2S-induced cytoprotection is not well understood, a growing body of evidence suggests that the effect of H_2S is mediated by induction of anti-oxidative (27,29,40) and anti-apoptotic pathways (40). However the mechanism by which H_2S orchestrates a cellular defense response is not well studied.

The key biochemical step for ISR is the induction of eIF2α phosphorylation, an evolutionarily conserved cytoprotective response, which has broad cellular consequences including translational and transcriptional reprograming (41,42). Phosphorylation of eIF2α at Ser51 is catalyzed by four kinases, GCN2, PERK, HRI and PKR, each responding to different stresses (42). Phosphorylation of eIF2α blocks global mRNA translation while translation of select cytoprotective proteins, including ATF4, continues via regulatory uORFs in their 5'-UTRs (42). ATF4 activates expression of stress response genes and promotes proteostasis via a feedback loop that involves induction of GADD34, a regulatory subunit of protein phosphatase-1 (PP1c), which dephosphorylates eIF2α-P. Low basal level of eIF2α-P in unstressed cells is maintained by the action of PP1c in complex with the constitutively expressed regulatory subunit CReP (43-45).

In this study, we tested the hypothesis that H_2S regulates the ISR signaling pathway. Herein we describe the cellular response to H_2S and show that exogenous H_2S or induction of its endogenous synthesis leads to increased eIF2α phosphorylation. H_2S-leads to increased eIF2α-P levels by inhibiting PP1c phosphatase via persulfidation, which in turn leads to transient suppression of global translation and activation of ATF4 expression.

RESULTS

H_2S induces phosphorylation of eIF2α- To test whether H_2S modulates eIF2α phosphorylation, we treated mouse embryonic fibroblast (MEF) cells and HeLa cells with 100 μM NaHS for 2 h. NaHS treatment resulted in an ~2.5-fold increase in eIF2α phosphorylation in both cell types while the total eIF2α levels did not change (Fig. 1a and b). The increase in eIF2α phosphorylation was evident as early as 1 h after H_2S exposure, and decayed to baseline levels after 8-12 h (Fig 1c,d). A 25 μM concentration of NaHS was sufficient to increase eIF2α-P levels and no further increase was seen at concentrations up to 200 μM (Fig. 1e,f). In comparison, the ER stress-inducing agent, tunicamycin (Tn) resulted in a more robust increase in eIF2α phosphorylation (Fig. 1a). However, repeated exposure to H_2S (100 μM NaHS added every 4 h) resulted in a gradual increase in eIF2α phosphorylation with no change in eIF2α level (Fig, 1g).

Next, we tested if induction of endogenous H_2S production elicits similar effects on eIF2α phosphorylation levels. We have recently described a regulatory switch whereby inhibition of CBS by CO increases H_2S production by CSE (46). We exploited this regulatory strategy by overexpressing heme oxygenase-2 (HO-2), a CO producing enzyme, in HEK293 cells. Transient overexpression of HO-2 increased endogenous H_2S levels, as detected in live cells using the fluorescent H_2S probe, 7-azido-4-methylcoumarin that was sensitive to propargylglycine, an inhibitor of CSE (Fig. 2a), and resulted in a 4-fold increase in basal eIF2α-P level compared to cells transfected with an empty plasmid (p=0.02) (Fig. 2b). We obtained similar results by overexpressing nitric oxide synthase (NOS), a source of NO, which also inhibits CBS activity (47) (Fig. 2d). While the increase in eIF2α-P levels in response to a single does of exogenous H_2S was transient, induction of endogenous H_2S production by HO-2 overexpression resulted in a persistent increase in eIF2α-P (compare Fig. 2b,c. with Fig. 1a,b). This result reveals that both induction of endogenous H_2S synthesis and exogenous H_2S addition are associated with increased eIF2α-P levels. To further test whether the increase in eIF2α-P level by overexpression of CO or NO producing enzymes is mediated by CBS inhibition, we analyzed eIF2α-P levels in liver tissue homogenates prepared from $CBS^{-/-}$ mice, described previously (48). A ~2-fold higher level of eIF2α-P levels was consistently seen in $CBS^{-/-}$ liver compared to wild type control (Fig. 2e,f)

Inhibition of global protein synthesis by H_2S-We tested whether H_2S-induced eIF2α phosphorylation leads to inhibition of protein translation. For this, we monitored incorporation of [^{35}S]-methionine into the protein pool in MEF cells (± 100 μM NaHS treatment) and in HEK293 cells transiently overexpressing HO-2 in the absence of exogenous H_2S. We observed a significant decrease in translation in H_2S-treated cells (p=0.007) and in HO-2 overexpressing HEK293 cells (p=0.005) compared to controls (Fig. 3a and b). Since exogenous H_2S increased eIF2α-P levels transiently (Fig. 1d), we determined whether the kinetics of translational suppression was correlated with this behavior. For this, we monitored the time-dependent changes in protein translation in MEF cells exposed to a single dose of H_2S (100 μM NaHS). H_2S-induced inhibition of protein synthesis was exerted over 4 h and returned to baseline levels over 8-12 h mirroring the pattern of H_2S-induced increase in eIF2α-P levels (Fig. 3c and Fig. 1c). This result is consistent with the involvement of H_2S-induced eIF2α phosphorylation in translational suppression.

Next, we tested whether H_2S induced ATF4 expression, which is associated with increased eIF2α-P levels and inhibition of global translation ATF4 was increased in MEF cells after a single dose of H_2S treatment (Fig. 4a), and in cells stably overexpressing HO-2, compared to control cells (Fig. 4b) confirming induction of ATF4 expression by H_2S.

Inactivation of protein phosphatase-1 by persulfidation-The transient increase in eIF2α phosphorylation levels in response to H_2S treatment can result from activation of one of the four upstream kinases and/or by inhibition of the phosphatase, PP1c. We hypothesized that the increase in eIF2α-P levels by H_2S results from inhibition of the basal activity of PP1c for the following reason. H_2S-induced increase in eIF2α-P levels was lower compared to the effect of ER stress inducing agents (Fig. 1a) and was independent of H_2S concentration between 25-200 μM NaHS (Fig. 1e). Additional increase in eIF2α-P levels required either repeated exposure to H_2S (Fig. 1g) or sustained H_2S overproduction (Fig 2b and c). These results suggested to us that the increase in eIF2α-P levels upon H_2S exposure is limited by its rate of basal phosphorylation.

To test our hypothesis, we expressed and purified recombinant human PP1c to ~95% purity and analyzed the effect of H_2S on dephosphorylation of eIF2α-P in extracts prepared from cells exposed to ER stress. Addition of PP1c to extracts reduced eIF2α-P

(p=0.007) while NaHS-treated PP1c had no effect (Fig. 5a and b). PP1c contains 13 cysteines including several reactive ones, Cys127, Cys273 and Cys291 (49). We hypothesized that the observed decrease in PP1c activity in the presence of H_2S was due to persulfidation, which was characterized by mass spectroscopic analysis. A single cysteine, corresponding to Cys127, was identified as being persulfidated (Fig. 6). To test whether Cys127 mediates the effect of H_2S on PP1c activity, we substituted C127 with serine. While PP1c-C127S efficiently dephosphorylated eIF2α in cell extracts (p=0.01), it was unresponsive to H_2S treatment (Fig. 5c and d) consistent with the importance of Cys127 in mediating the H_2S effect. To further validate these results, we overexpressed wild type and C127S-PP1c in HEK293 cells. Overexpression of wild type and mutant PP1c significantly reduced eIf2α-P levels (Fig. 5e and f) as expected (43,44). Treatment of these cells with 100 μM H_2S increased eIF2α-P level in cells overexpressing wild type PP1c but not in cells overexpressing C127S-PP1c (Fig. 5e) confirming that Cys127 is required to mediate H_2S inhibition of PP1c activity. Interestingly, H_2S had no effect on dephosphorylation when *p*-nitrophenyl phosphate or a phospho-peptide corresponding to residues 45-56 of eIF2α (ILLSEL(p-Ser)RRRIR), was used as substrates (data not shown). This difference in H_2S effects on PP1c presumably results from differences in its interaction between the phosphopeptide and full-length protein substrates as also demonstrated for eIF2α phosphorylation, which requires at least 80 amino acids from the N-terminus (50).

Involvement of PERK kinase in H_2S-induced phosphorylation of eIF2α-H_2S reportedly inhibits PTP1B phosphatase during ER stress (51). PTP1B dephosphorylates the PERK kinase, an ER stress sensor that autophosphorylates and induces the PERK branch of the ISR during ER stress by phosphorylating eIF2α. We tested if H_2S-mediated increase in eIF2α-P levels was contributed by increased phosphorylation of PERK due to inhibition of PTP1B by H_2S. For this we analyzed the effect of H_2S on eIF2α-P levels in $Perk^{-/-}$, and $Perk^{+/+}$ MEF cells. H_2S treatment for 1 h resulted in an ~2-fold increase in eIF2α-P levels in both wild type (p=0.02) and $Perk^{-/-}$ MEF cells (p= 0.009) (Fig. 7a and b). These results were mirrored by changes in translation rates measured in the presence and absence of H_2S in $Perk^{+/+}$ and $Perk^{-/-}$ MEF cells (Fig. 7c). These results indicate that H_2S-induced increase in eIF2α-P level is independent of PERK activation

Effect of HO-2 overexpression on stress resistance-We determined the viability of three cell lines exposed to H_2S for 2 h prior to induction of ER stress with thapsigargin. H_2S protected cells from ER stress-induced cell death in all cell lines (Fig. 8a) consistent with previous reports (34-37). H_2S treatment alone in the absence of stress had no effect on cell viability (Fig. 8b). We tested the effect of sustained high H_2S levels in cells stably overexpressing HO-2. While these cells are more resistant to transient stress induced by thapsigargin (Fig.8a), they are slow growing and die off after 4-6 passages.

The transient pre-emptive induction of eIF2α phosphorylation is known to be cytoprotective for further stress (52). Therefore, we examined eIF2α-P levels in response to ER stress induced with Tg in cells with prior H_2S exposure. The increase in eIF2α-P levels upon Tg treatment was significantly lower in H_2S pretreated cells compared to Tg alone treatment (Fig. 8c,d) suggesting that H_2S increases cellular threshold to stress. This is consistent with the report that the increase in eIF2α-P levels induced by a mild transient stress in neuroblastoma cells prevents further increase in eIF2α-P levels in response to a subsequent acute stress (53). Our results suggest that the cytoprotective function of H_2S is in part mediated by inhibition of PP1c and transient modulation of the ISR components, eIF2α-P phosphorylation and global protein synthesis, (52).

DISCUSSION

In this study, we have characterized an H_2S signaling pathway using a cellular model

system where endogenousH_2S production was induced by overexpressing HO-2. Our results indicate that H_2S is a physiological modulator of eIF2α phosphorylation statusand that it exerts its effect via a mechanism involving persulfidation and concomitant inhibition of PP1c. Phosphorylation of eIF2α is typically induced under stress conditions by activation of upstream kinases to guard against dysregulation of cellular homeostasis. However, the existence of signaling pathways to transiently induce eIF2α phosphorylation in the absence of overt stress is largely unexplored. Herein, we show that H_2S-induced inhibition of PP1c provides an alternative route to modulate eIF2α-P levels independent of upstream kinases. We propose that while a transient increase in H_2S production induces an acute response, which is consistent with its cytoprotective effects, continuous exposure results in persistent increase in eIF2α-P levels but is tolerated in cells due to the presence of an efficient H_2S oxidation pathway present in mitochondria. Consistent with this model, disruption of the first sulfide oxidation pathway enzyme in *C. elegans,* leads to death upon H_2S exposure resulting from both ER and mitochondrial stress (54).

A cytoprotective effect for H_2S-induced inhibition of PP1c leading to a transient increase in basal eIF2α-P levels is consistent with other reports. For instance, inhibition of PP1c activity by knocking down CReP, activates the ISR and is cytoprotective against stressors including oxidative and ER stress (43). Similarly, inhibition of PP1c interaction with the regulatory subunits by salubrinal (55) or by mutagenesis (44), and by GADD34 knockout (56) increases eIF2α-P levels, inhibits translation and, in some systems, has a protective role against stress (43,55,56). Our results might be relevant to understanding the protective effect of H_2S on protein metabolism in response to hypoxia-induced stress as discussed below (57).

PP1c is rich in cysteine residues and contains several reactive ones. Cys273 is critical for activity and microcystin, an inhibitor of PP1c, functions by binding covalently to the sulfur in Cys273 (49,58). In the crystal structure of PP1c, Cys127 is oxidized to sulfinic or sulfonic acid and Cys291 forms a mixed disulfide with mercaptoethanol (49). Our results validate that Cys127 in PP1c is a target of persulfidation, which was initially picked up in a persulfide proteomic analysis under ER stress conditions that is accompanied by increased H_2S synthesis (39). We predict that PP1c activity is sensitive to cysteine modifications, and its inhibition by persulfidation results in increased eIF2α-P levels and to modulation of global translation.

PP1c associates with a variety of regulatory subunits that dictate target specificity (59). While the dependence of H_2S effect on the identity of the regulatory domains remains to be demonstrated, our model is consistent with the reported effect of H_2S on increasing phosphorylation levels of AMP-activated protein kinase (60), which is dephosphorylated by PP1c in complex with the regulatory subunit R6 (61). AMP-activated protein kinase functions as an energy sensor and its phosphorylation under hypoxia activates the AMPK/TSC2/Rheb/mTOR signaling pathway, which inhibits mTOR activity. These changes lead to suppression of the initiation and elongation phases of translation (62,63). Although, it is not understood how H_2S treatment modulates this signaling network during hypoxia, we speculate that H_2S-induced inhibition of PPIc activity might increase AMPK phosphorylation for inhibition of eIF2B activity.

In summary, we have shown that transient exposure of cells to H_2S leads to increased eIF2α phosphorylation by PP1c persulfidation at Cys127, which leads to its inhibition, This study reveals a previously unknown mode of regulation for eIF2α–P level that may underlie the cytoprotective effects of H_2S. The ISR/ATF4 program mediates metabolic reprogramming of cells exposed to ER stress via H_2S-mediated protein persulfidation (39). The current findings suggest that H_2S might also contribute to the outcome of ISR in part by modulating translational recovery required for transcriptional reprogramming and adaptation (64,65). Translational recovery depends on

the phosphorylation status of eIF2α and is critical in most chronic stress conditions as uncontrolled translational recovery decreases survival of stressed cells (39,66,67). Our data suggest that inhibition of PP1c by H_2S can potentially dampen translational recovery and be important in delaying the onset of diseases involving chronic stress.

EXPERIMENTAL PROCEDURES

Materials-Rabbit polyclonal anti-eIF2α (Cat # 9722), rabbit monoclonal anti-PERK (Cat # 3192), and rabbit monoclonal anti-PERK-P (Cat # 3179) were purchased from Cell Signaling Tec. Rabbit monoclonal anti-eIF2α-P (Cat # ab32157) was purchased from Abcam. Rabbit polyclonal anti-HO-2 (Cat LS-C48375) was purchased from LS-BIO. Rabbit polyclonal anti-ATF4 (Cat # cs-200) was purchased from Santa Cruz Biotechnology, Inc. Rabbit polyclonal anti-PP1c (Cat # 55150-1-AP) was purchased from Proteintech. All other chemicals were purchased from Sigma unless otherwise noted.

Cell Culture-ATF$^{+/+}$ and ATF4$^{-/-}$ MEFs were obtained from Dr. Ronald Wek (Indiana University School of Medicine) and were described previously (41,68). HEK293, RWPE (prostate cells), and HeLa, cells were grown in DMEM medium. LNCaP cells (prostate cancer cells) were grown in RPMI 1640 media. Perk$^{+/+}$ MEF, and Perk$^{-/-}$ MEF cells were grown in DMEM medium. ATF4$^{-/-}$ MEF cells were grown in DMEM medium supplemented with 1% nonessential amino acid solution (NEAA, Life Technologies) and 55 μM mercaptoethanol (Life Technologies). All media were supplemented with 10 % FBS and penicillin-streptomycin (100 units/ml and 100 μg/ml, respectively). Transient transfections were performed using the Xtreme Gene HP transfection reagent (Roche) according to the manufacturer's protocol. HeLa cells stably expressing HO-2 was obtained by selection with geneticin, 0.6 μg/mL. ER stress was induced with thapsigargin or tunicamycin to the medium at a final concentration from 0.5 to 1 μM and 5 μg/mL, respectively, as specified in the figure legends.

Metabolic labeling and determination of protein translation rate-Cells were grown in either 6 cm plates or in 12-well plates to a confluency of 80%. Then, they were labeled with 15 or 30 μCi/mL [^{35}S]-methionine (Perkin Elmer), and continued to grow for 1-2 h depending on the experiment. Fresh medium was added to plates 1 h before radiolabel addition. At the end of the labeling time, cells were washed twice with PBS and scraped off the plates in RIPA buffer. After two freeze/thaw cycles, 10 % (v/v) of trichloroacetic acid (TCA) was added to precipitate proteins. Aliquots from extracts were used to measure protein concentration. The protein precipitate was washed twice with 5% TCA and dissolved in 200 μL of 1 M NaOH and the radioactivity was counted in a liquid scintillation counter. Radioactivity was normalized to protein concentration measured using Bradford reagent (Bio-Rad) with bovine serum albumin as the standard. For radioactive gels, extracts were denatured in SDS dye loading buffer and boiled for 5 min before electrophoresis. Equal amounts of protein were loaded in each well. Radioactive gels were dried in a gel dryer attached to a vacuum pump, placed on a phosphor storage screen cassette for 24 h, and imaged on a STORM 860 phosphorimager. Autoradiograms were quantified using the software ImageJ.

Western blotting analysis-Cells were washed three times with PBS on ice and scraped in 50 mM Tris, pH 7.4, containing 0.1% Triton X-100, complete protease inhibitor cocktail (Sigma) or in RIPA buffer supplemented with protease inhibitor cocktail. Extracts were incubated on ice for 30 min before centrifuging at 13,000 g for 10 min at 4 °C. Aliquots of supernatants were added to SDS denaturing buffer and boiled for 5-10 min. Equal amounts of proteins were separated on 10-12 % SDS PAGE gel and then transferred to a PVDF membrane. Membranes were blocked with 5 % nonfat dry milk in TTBS (Tris-buffered saline containing 0.1 %Tween-20) for 1 h at room temperature with shaking, and washed four times with

TTBS before overnight incubation with the primary antibody at 4 °C. Membranes were washed for 4-5 times, 20 min each, with TTBS and then incubated with the secondary antibody conjugated to horseradish peroxidase for 1 h at room temperature. Signal intensities for specific proteins were estimated using NIH ImageJ software. Antibody dilutions were as follows: anti-eIF2α: 1:1000, anti-eIF2α: 1:1000, anti-HO-2: 1: 1000, anti-PP1c: 1:1000, and anti-ATF4: 1:500.

Western based eIF2α dephosphorylation assay-Cells were treated with thapsigargin for >24 h to induce eIF2α phosphorylation. Dephosphoylation of eIF2α was performed in 50 μl reaction mixture containing 50 mM Tris, pH 7.4, 100 mM KCl and 4 mM $MgCl_2$ and 50-100 μg of protein from cell extracts prepared as described above from Tg-treated cells but without protease inhibitors. Reactions were started by adding 5-10 μg of purified wild type or mutant PP1c with or without H_2S pretreatment (250 μM final) and incubated at room temperature for 10 min. At the end of the incubation time, SDS denaturing buffer was added to the reaction mixtures and boiled for 5 min at 95 °C. Proteins were separated on a 10% SDS gel and transferred to PVDF membrane for western blotting analysis as described above to detect eIF2α and eIF2α-P levels. Signal intensities for eIF2α were quantified from three independent experiments.

Fluorescence microscopy-H_2S was visualized in HEK293 cells transfected with mammalian expression construct for HO-2 or with an empty plasmid using 7-Azido-4-methylcoumarin as described previously (69). Briefly, 30-36 h post-transfection, 7-Azido-4-methylcoumarin was added to the culture medium to a final concentration of 50 μM and incubation was continued for 30 min. Then, the cells were washed three times with PBS and visualized using an IX70 inverted microscope, connected with Photometrics coolSnap HQ2 camera, using 720 nm laser excitation. Metamorph software was used to acquire and analyze images. Propargylglycine (PPG), an inhibitor of the H_2S producing enzyme, CSE, was added 6 h prior to imaging at 2 mM final concentration.

Cloning, expression and purification of PP1c–The mammalian expression vector containing PP1c, pEZ-M01, was purchased from GeneCopoeia (Rockville, MD). The PP1c coding region was PCR amplified using the forward (5´-GGAAGGAGTTCGACATATGGCGGATTTAGATAAACTCAACATCG) and reverse (5´-GCGGCCGCACTCGAGCTATTTCTTTGCTTGCTTTGTGATCATAC) primers containing the Xho1 and Nde1 restriction sites, which were used for subcloning into the pET28b bacterial expression vector to generate the expression construct pET28b-PP1c. *E. coli* BL21 (DE3) cells transformed with the pET28b-PP1c construct were grown overnight at 37 °C in 100 mL of LB media containing kanamycin (50 μg/mL) and used to inoculate 6 liter LB media. Cells were grown at 25 °C. Expression of PP1c was induced with isopropyl β-D-thiogalactopyranoside (25 mg/L) when the OD_{600} reached 0.5. Cells were harvested after 16 h and fresh or frozen cell pellets were suspended in 200 mL lysis buffer containing, 20 mM sodium phosphate (pH=7.4), 150 mg lysozyme 10 mM $MgCl_2$, 500 mM NaCl, 20 mg DNAase and 10% glycerol. The cell suspension was stirred at 4 °C for 30 min and then sonicated at a power setting of 7 for 10 min in 30 sec intervals separated by 1 min cooling. The sonicate was centrifuged at 17,000 x *g* for 30 min to obtain the soluble fraction. The N-terminal His-tagged PP1c was affinity purified using a Ni-NTA column in 20 mM sodium phosphate buffer, pH 7.4, 500 mM NaCl, 10% glycerol. Further purification was achieved by gel filtration chromatography using a pre-packed Hiload 16/60 Superdex 200 column (GE Healthcare) using the same buffer.

Mass Spectrometry-Recombinant PP1γ (20 μg) was treated with NaHS (1 mM) at room temperature for 30 min and then incubated with the thiol-blocking buffer containing 20 mM NEM for 30 min. NEM-alkylated PP1γ was subjected to a non-reducing SDS gel and stained with Coomassie blue. The PP1γ protein band was

excised and digested with trypsin and chymotrypsin. The peptide samples were analyzed by capillary column LC-tandem MS and the CID spectra searched against the human reference sequence database using the program Mascot and more specifically against the protein sequences with the program Sequest. All analyses utilized the standard LC gradient from 2 to 70% acetonitrile in 110 min.

Cell viability analysis-Since H_2S can impact metabolic rate and energy production, we used the trypan blue assay for staining and counting live and dead cells under the microscope using a hemocytometer. Flow cytometry was used for MEF to determine the effect of H_2S on cell viability using propidium iodide (Calbiochem) to stain dead cells. Cells were harvested by trypsinization and washed twice with PBS. To the cell suspensions, 1% BSA (w/v) and propidioum iodide (~1 μM final) were added for flow cytometry or alternatively, mixed with trypan blue for counting under the microscope. The data are presented as percent dead or live cells.

Statistical analysis-The statistical significance of observed differences was evaluated using Paired t test.

Acknowledgements: We thank Dr. Ronald Wek (Indiana University School of Medicine) for providing $ATF4^{-/-}$ and $ATF4^{+/+}$ MEF cells, Dr. Stephen Ragsdale (University of Michigan Medical School) for providing us with the mammalian expression construct for HO-2, Dr. Warren Kruger (Fox Chase Cancer Center, Philadelphia, PA) for providing liver tissues from Cbs−/− (Tg-I278T) and wild-type mice and Jing Wu (Case Western Reserve University) for maintaining MEF cells. This work was supported by an American Heart Association grant (13SDG17070096 to OK), NIH grants (DK53307 and DK60596 to MH and HL58984 and GM112455 to RB) and an ADA postdoc fellowship 1-17-PDF-129 to XHG.

Conflict of interest: The authors declare no conflict of interest.

Author contributions: VY performed majority of the experiments and analyzed the data. X-HG contributed with his expertise in preparing samples for detection of PP1c persulfidation. BW performed the mass spectroscopy analysis with LC-MS/MS. MH contributed to designing of study related to ISR, data analysis and manuscript preparation. RB contributed to data analysis and helped in manuscript preparation. OK conceived and designed the study, analyzed and interpreted the data, performed experiments and prepared the manuscript. All authors approved the final version of the manuscript.

REFERENCES

1. Lavu, M., Bhushan, S., and Lefer, D. J. (2011) Hydrogen sulfide-mediated cardioprotection: mechanisms and therapeutic potential. *Clinical science* **120**, 219-229
2. Gong, Q. H., Shi, X. R., Hong, Z. Y., Pan, L. L., Liu, X. H., and Zhu, Y. Z. (2011) A new hope for neurodegeneration: possible role of hydrogen sulfide. *J Alzheimers Dis* **24 Suppl 2**, 173-182
3. Abe, K., and Kimura, H. (1996) The possible role of hydrogen sulfide as an endogenous neuromodulator. *J Neurosci* **16**, 1066-1071
4. Shibuya, N., Tanaka, M., Yoshida, M., Ogasawara, Y., Togawa, T., Ishii, K., and Kimura, H. (2009) 3-Mercaptopyruvate sulfurtransferase produces hydrogen sulfide and bound sulfane sulfur in the brain. *Antioxidants & redox signaling* **11**, 703-714
5. Yadav, P. K., Yamada, K., Chiku, T., Koutmos, M., and Banerjee, R. (2013) Structure and kinetic analysis of H2S production by human mercaptopyruvate sulfurtransferase. *The Journal of biological chemistry* **288**, 20002-20013
6. Hildebrandt, T. M., and Grieshaber, M. K. (2008) Three enzymatic activities catalyze the oxidation of sulfide to thiosulfate in mammalian and invertebrate mitochondria. *The FEBS journal* **275**, 3352-3361
7. Beauchamp, R. O., Bus, J. S., Popp, J. A., Boreiko, C. J., and Andjelkovich, D. A. (1984) A Critical-Review of the Literature on Hydrogen-Sulfide Toxicity. *Crc Cr Rev Toxicol* **13**, 25-97
8. Vorobets, V. S., Kovach, S. K., and Kolbasov, G. Y. (2002) Distribution of ion species and formation of ion pairs in concentrated polysulfide solutions in photoelectrochemical transducers. *Russ J Appl Chem+* **75**, 229-234
9. Mathai, J. C., Missner, A., Kugler, P., Saparov, S. M., Zeidel, M. L., Lee, J. K., and Pohl, P. (2009) No facilitator required for membrane transport of hydrogen sulfide. *P Natl Acad Sci USA* **106**, 16633-16638
10. Mustafa, A. K., Gadalla, M. M., Sen, N., Kim, S., Mu, W., Gazi, S. K., Barrow, R. K., Yang, G., Wang, R., and Snyder, S. H. (2009) H2S signals through protein S-sulfhydration. *Science signaling* **2**, ra72
11. Kabil, O., and Banerjee, R. (2014) Enzymology of H2S biogenesis, decay and signaling. *Antioxidants & redox signaling* **20**, 770-782
12. Hosoki, R., Matsuki, N., and Kimura, H. (1997) The possible role of hydrogen sulfide as an endogenous smooth muscle relaxant in synergy with nitric oxide. *Biochemical and biophysical research communications* **237**, 527-531
13. Zhao, W., Zhang, J., Lu, Y., and Wang, R. (2001) The vasorelaxant effect of H(2)S as a novel endogenous gaseous K(ATP) channel opener. *The EMBO journal* **20**, 6008-6016
14. Yang, G., Wu, L., Jiang, B., Yang, W., Qi, J., Cao, K., Meng, Q., Mustafa, A. K., Mu, W., Zhang, S., Snyder, S. H., and Wang, R. (2008) H_2S as a physiologic vasorelaxant: hypertension in mice with deletion of cystathionine gamma-lyase. *Science* **322**, 587-590
15. Ali, M. Y., Ping, C. Y., Mok, Y. Y., Ling, L., Whiteman, M., Bhatia, M., and Moore, P. K. (2006) Regulation of vascular nitric oxide in vitro and in vivo; a new role for endogenous hydrogen sulphide? *British journal of pharmacology* **149**, 625-634
16. Mustafa, A. K., Sikka, G., Gazi, S. K., Steppan, J., Jung, S. M., Bhunia, A. K., Barodka, V. M., Gazi, F. K., Barrow, R. K., Wang, R., Amzel, L. M., Berkowitz, D. E., and Snyder, S. H. (2011) Hydrogen sulfide as endothelium-derived hyperpolarizing factor sulfhydrates potassium channels. *Circulation research* **109**, 1259-1268
17. Geng, B., Yang, J., Qi, Y., Zhao, J., Pang, Y., Du, J., and Tang, C. (2004) H2S generated by heart in rat and its effects on cardiac function. *Biochemical and biophysical research communications* **313**, 362-368

18. Cheng, Y., Ndisang, J. F., Tang, G., Cao, K., and Wang, R. (2004) Hydrogen sulfide-induced relaxation of resistance mesenteric artery beds of rats. *American journal of physiology. Heart and circulatory physiology* **287**, H2316-2323
19. Dello Russo, C., Tringali, G., Ragazzoni, E., Maggiano, N., Menini, E., Vairano, M., Preziosi, P., and Navarra, P. (2000) Evidence that hydrogen sulphide can modulate hypothalamo-pituitary-adrenal axis function: in vitro and in vivo studies in the rat. *J Neuroendocrinol* **12**, 225-233
20. Elrod, J. W., Calvert, J. W., Morrison, J., Doeller, J. E., Kraus, D. W., Tao, L., Jiao, X., Scalia, R., Kiss, L., Szabo, C., Kimura, H., Chow, C. W., and Lefer, D. J. (2007) Hydrogen sulfide attenuates myocardial ischemia-reperfusion injury by preservation of mitochondrial function. *Proc Natl Acad Sci U S A* **104**, 15560-15565
21. Nicholson, C. K., and Calvert, J. W. (2010) Hydrogen sulfide and ischemia-reperfusion injury. *Pharmacological research* **62**, 289-297
22. Ansari, S. B., and Kurian, G. A. (2016) Hydrogen sulfide modulates sub-cellular susceptibility to oxidative stress induced by myocardial ischemic reperfusion injury. *Chemico-biological interactions* **252**, 28-35
23. Calvert, J. W., Elston, M., Nicholson, C. K., Gundewar, S., Jha, S., Elrod, J. W., Ramachandran, A., and Lefer, D. J. (2010) Genetic and pharmacologic hydrogen sulfide therapy attenuates ischemia-induced heart failure in mice. *Circulation* **122**, 11-19
24. Barr, L. A., Shimizu, Y., Lambert, J. P., Nicholson, C. K., and Calvert, J. W. (2015) Hydrogen sulfide attenuates high fat diet-induced cardiac dysfunction via the suppression of endoplasmic reticulum stress. *Nitric Oxide-Biol Ch* **46**, 145-156
25. Polhemus, D. J., Kondo, K., Bhushan, S., Bir, S. C., Kevil, C. G., Murohara, T., Lefer, D. J., and Calvert, J. W. (2013) Hydrogen Sulfide Attenuates Cardiac Dysfunction After Heart Failure Via Induction of Angiogenesis. *Circ-Heart Fail* **6**, 1077-1086
26. Kondo, K., Bhushan, S., King, A. L., Prabhu, S. D., Hamid, T., Koenig, S., Murohara, T., Predmore, B. L., Gojon, G., Gojon, G., Wang, R., Karusula, N., Nicholson, C. K., Calvert, J. W., and Lefer, D. J. (2013) H2S Protects Against Pressure Overload-Induced Heart Failure via Upregulation of Endothelial Nitric Oxide Synthase. *Circulation* **127**, 1116-+
27. Kimura, Y., and Kimura, H. (2004) Hydrogen sulfide protects neurons from oxidative stress. *Faseb J* **18**, 1165-+
28. Kimura, Y., Dargusch, R., Schubert, D., and Kimura, H. (2006) Hydrogen sulfide protects HT22 neuronal cells from oxidative stress. *Antioxidants & redox signaling* **8**, 661-670
29. Kimura, Y., Goto, Y., and Kimura, H. (2010) Hydrogen sulfide increases glutathione production and suppresses oxidative stress in mitochondria. *Antioxidants & redox signaling* **12**, 1-13
30. Whiteman, M., Armstrong, J. S., Chu, S. H., Jia-Ling, S., Wong, B. S., Cheung, N. S., Halliwell, B., and Moore, P. K. (2004) The novel neuromodulator hydrogen sulfide: an endogenous peroxynitrite 'scavenger'? *Journal of neurochemistry* **90**, 765-768
31. Whiteman, M., Cheung, N. S., Zhu, Y. Z., Chu, S. H., Siau, J. L., Wong, B. S., Armstrong, J. S., and Moore, P. K. (2005) Hydrogen sulphide: a novel inhibitor of hypochlorous acid-mediated oxidative damage in the brain? *Biochemical and biophysical research communications* **326**, 794-798
32. Tang, X. Q., Yang, C. T., Chen, J., Yin, W. L., Tian, S. W., Hu, B., Feng, J. Q., and Li, Y. J. (2008) Effect of hydrogen sulphide on beta-amyloid-induced damage in PC12 cells. *Clin Exp Pharmacol P* **35**, 180-186
33. Li, X. H., Deng, Y. Y., Li, F., Shi, J. S., and Gong, Q. H. (2016) Neuroprotective effects of sodium hydrosulfide against beta-amyloid-induced neurotoxicity. *International journal of molecular medicine* **38**, 1152-1160

34. Xie, L., Tiong, C. X., and Bian, J. S. (2012) Hydrogen sulfide protects SH-SY5Y cells against 6-hydroxydopamine-induced endoplasmic reticulum stress. *Am J Physiol-Cell Ph* **303**, C81-C91
35. Li, X., Zhang, K. Y., Zhang, P., Chen, L. X., Wang, L., Xie, M., Wang, C. Y., and Tang, X. Q. (2014) Hydrogen sulfide inhibits formaldehyde-induced endoplasmic reticulum stress in PC12 cells by upregulation of SIRT-1. *PLoS One* **9**, e89856
36. Wei, H. L., Zhang, R. Y., Jin, H. F., Liu, D. E., Tang, X. Y., Tang, C. S., and Du, J. B. (2010) Hydrogen Sulfide Attenuates Hyperhomocysteinemia-Induced Cardiomyocytic Endoplasmic Reticulum Stress in Rats. *Antioxidants & redox signaling* **12**, 1079-1091
37. Ying, R., Wang, X. Q., Yang, Y., Gu, Z. J., Mai, J. T., Qiu, Q., Chen, Y. X., and Wang, J. F. (2016) Hydrogen sulfide suppresses endoplasmic reticulum stress-induced endothelial-to-mesenchymal transition through Src pathway. *Life Sci* **144**, 208-217
38. Zeisberg, E. M., Tarnavski, O., Zeisberg, M., Dorfman, A. L., McMullen, J. R., Gustafsson, E., Chandraker, A., Yuan, X. L., Pu, W. T., Roberts, A. B., Neilson, E. G., Sayegh, M. H., Izumo, S., and Kalluri, R. (2007) Endothelial-to-mesenchymal transition contributes to cardiac fibrosis. *Nat Med* **13**, 952-961
39. Gao, X. H., Krokowski, D., Guan, B. J., Bederman, I., Majumder, M., Parisien, M., Diatchenko, L., Kabil, O., Willard, B., Banerjee, R., Wang, B., Bebek, G., Evans, C. R., Fox, P. L., Gerson, S. L., Hoppel, C., Liu, M., Arvan, P., and Hatzoglou, M. (2015) Quantitative H_2S-mediated protein sulfhydration reveals metabolic reprogramming during the Integrated Stress Response. *eLife* **4**
40. Jha, S., Calvert, J. W., Duranski, M. R., Ramachandran, A., and Lefer, D. J. (2008) Hydrogen sulfide attenuates hepatic ischemia-reperfusion injury: role of antioxidant and antiapoptotic signaling. *American journal of physiology. Heart and circulatory physiology* **295**, H801-806
41. Harding, H. P., Zhang, Y., Zeng, H., Novoa, I., Lu, P. D., Calfon, M., Sadri, N., Yun, C., Popko, B., Paules, R., Stojdl, D. F., Bell, J. C., Hettmann, T., Leiden, J. M., and Ron, D. (2003) An integrated stress response regulates amino acid metabolism and resistance to oxidative stress. *Molecular cell* **11**, 619-633
42. Baird, T. D., and Wek, R. C. (2012) Eukaryotic Initiation Factor 2 Phosphorylation and Translational Control in Metabolism. *Adv Nutr* **3**, 307-321
43. Jousse, C., Oyadomari, S., Novoa, I., Lu, P., Zhang, Y., Harding, H. P., and Ron, D. (2003) Inhibition of a constitutive translation initiation factor 2alpha phosphatase, CReP, promotes survival of stressed cells. *J Cell Biol* **163**, 767-775
44. Novoa, I., Zeng, H. Q., Harding, H. P., and Ron, D. (2001) Feedback inhibition of the unfolded protein response by GADD34-mediated dephosphorylation of eIF2 alpha. *Journal of Cell Biology* **153**, 1011-1021
45. Bollen, M., Peti, W., Ragusa, M. J., and Beullens, M. (2010) The extended PP1 toolkit: designed to create specificity. *Trends Biochem Sci* **35**, 450-458
46. Kabil, O., Yadav, V., and Banerjee, R. (2016) Heme-dependent Metabolite Switching Regulates H2S Synthesis in Response to Endoplasmic Reticulum (ER) Stress. *The Journal of biological chemistry* **291**, 16418-16423
47. Taoka, S., and Banerjee, R. (2001) Characterization of NO binding to human cystathionine beta-synthase: possible implications of the effects of CO and NO binding to the human enzyme. *J Inorg Biochem* **87**, 245-251
48. Gupta, S., Kuhnisch, J., Mustafa, A., Lhotak, S., Schlachterman, A., Slifker, M. J., Klein-Szanto, A., High, K. A., Austin, R. C., and Kruger, W. D. (2009) Mouse models of cystathionine beta-synthase deficiency reveal significant threshold effects of hyperhomocysteinemia. *Faseb J* **23**, 883-893

49. Goldberg, J., Huang, H. B., Kwon, Y. G., Greengard, P., Nairn, A. C., and Kuriyan, J. (1995) Three-dimensional structure of the catalytic subunit of protein serine/threonine phosphatase-1. *Nature* **376**, 745-753
50. Majumder, M., Mitchell, D., Merkulov, S., Wu, J., Guan, B. J., Snider, M. D., Krokowski, D., Yee, V. C., and Hatzoglou, M. (2015) Residues required for phosphorylation of translation initiation factor eIF2alpha under diverse stress conditions are divergent between yeast and human. *Int J Biochem Cell Biol* **59**, 135-141
51. Krishnan, N., Fu, C., Pappin, D. J., and Tonks, N. K. (2011) H2S-Induced sulfhydration of the phosphatase PTP1B and its role in the endoplasmic reticulum stress response. *Science signaling* **4**, ra86
52. Lu, P. D., Jousse, C., Marciniak, S. J., Zhang, Y., Novoa, I., Scheuner, D., Kaufman, R. J., Ron, D., and Harding, H. P. (2004) Cytoprotection by pre-emptive conditional phosphorylation of translation initiation factor 2. *The EMBO journal* **23**, 169-179
53. Shelkovnikova, T. A., Dimasi, P., Kukharsky, M. S., An, H., Quintiero, A., Schirmer, C., Buee, L., Galas, M. C., and Buchman, V. L. (2017) Chronically stressed or stress-preconditioned neurons fail to maintain stress granule assembly. *Cell Death Dis* **8**, e2788
54. Horsman, J. W., and Miller, D. L. (2016) Mitochondrial Sulfide Quinone Oxidoreductase Prevents Activation of the Unfolded Protein Response in Hydrogen Sulfide. *The Journal of biological chemistry* **291**, 5320-5325
55. Boyce, M., Bryant, K. F., Jousse, C., Long, K., Harding, H. P., Scheuner, D., Kaufman, R. J., Ma, D., Coen, D. M., Ron, D., and Yuan, J. (2005) A selective inhibitor of eIF2alpha dephosphorylation protects cells from ER stress. *Science* **307**, 935-939
56. Marciniak, S. J., Yun, C. Y., Oyadomari, S., Novoa, I., Zhang, Y., Jungreis, R., Nagata, K., Harding, H. P., and Ron, D. (2004) CHOP induces death by promoting protein synthesis and oxidation in the stressed endoplasmic reticulum. *Genes Dev* **18**, 3066-3077
57. Fawcett, E. M., Hoyt, J. M., Johnson, J. K., and Miller, D. L. (2015) Hypoxia disrupts proteostasis in Caenorhabditis elegans. *Aging Cell* **14**, 92-101
58. Pereira, S. R., Vasconcelos, V. M., and Antunes, A. (2013) Computational study of the covalent bonding of microcystins to cysteine residues--a reaction involved in the inhibition of the PPP family of protein phosphatases. *The FEBS journal* **280**, 674-680
59. Cohen, P. T. (2002) Protein phosphatase 1--targeted in many directions. *J Cell Sci* **115**, 241-256
60. Lee, H. J., Mariappan, M. M., Feliers, D., Cavaglieri, R. C., Sataranatarajan, K., Abboud, H. E., Choudhury, G. G., and Kasinath, B. S. (2012) Hydrogen sulfide inhibits high glucose-induced matrix protein synthesis by activating AMP-activated protein kinase in renal epithelial cells. *The Journal of biological chemistry* **287**, 4451-4461
61. Garcia-Haro, L., Garcia-Gimeno, M. A., Neumann, D., Beullens, M., Bollen, M., and Sanz, P. (2010) The PP1-R6 protein phosphatase holoenzyme is involved in the glucose-induced dephosphorylation and inactivation of AMP-activated protein kinase, a key regulator of insulin secretion, in MIN6 beta cells. *Faseb J* **24**, 5080-5091
62. Arsham, A. M., Howell, J. J., and Simon, M. C. (2003) A novel hypoxia-inducible factor-independent hypoxic response regulating mammalian target of rapamycin and its targets. *The Journal of biological chemistry* **278**, 29655-29660
63. Liu, L., Cash, T. P., Jones, R. G., Keith, B., Thompson, C. B., and Simon, M. C. (2006) Hypoxia-induced energy stress regulates mRNA translation and cell growth. *Molecular cell* **21**, 521-531
64. Novoa, I., Zhang, Y., Zeng, H., Jungreis, R., Harding, H. P., and Ron, D. (2003) Stress-induced gene expression requires programmed recovery from translational repression. *The EMBO journal* **22**, 1180-1187

65. Kojima, E., Takeuchi, A., Haneda, M., Yagi, A., Hasegawa, T., Yamaki, K., Takeda, K., Akira, S., Shimokata, K., and Isobe, K. (2003) The function of GADD34 is a recovery from a shutoff of protein synthesis induced by ER stress: elucidation by GADD34-deficient mice. *Faseb J* **17**, 1573-1575
66. Han, J., Back, S. H., Hur, J., Lin, Y. H., Gildersleeve, R., Shan, J., Yuan, C. L., Krokowski, D., Wang, S., Hatzoglou, M., Kilberg, M. S., Sartor, M. A., and Kaufman, R. J. (2013) ER-stress-induced transcriptional regulation increases protein synthesis leading to cell death. *Nat Cell Biol* **15**, 481-490
67. Krokowski, D., Jobava, R., Guan, B. J., Farabaugh, K., Wu, J., Majumder, M., Bianchi, M. G., Snider, M. D., Bussolati, O., and Hatzoglou, M. (2015) Coordinated Regulation of the Neutral Amino Acid Transporter SNAT2 and the Protein Phosphatase Subunit GADD34 Promotes Adaptation to Increased Extracellular Osmolarity. *The Journal of biological chemistry* **290**, 17822-17837
68. Jiang, H. Y., Wek, S. A., McGrath, B. C., Lu, D., Hai, T., Harding, H. P., Wang, X., Ron, D., Cavener, D. R., and Wek, R. C. (2004) Activating transcription factor 3 is integral to the eukaryotic initiation factor 2 kinase stress response. *Mol Cell Biol* **24**, 1365-1377
69. Chen, B., Li, W., Lv, C., Zhao, M., Jin, H., Jin, H., Du, J., Zhang, L., and Tang, X. (2013) Fluorescent probe for highly selective and sensitive detection of hydrogen sulfide in living cells and cardiac tissues. *Analyst* **138**, 946-951

Figure 1

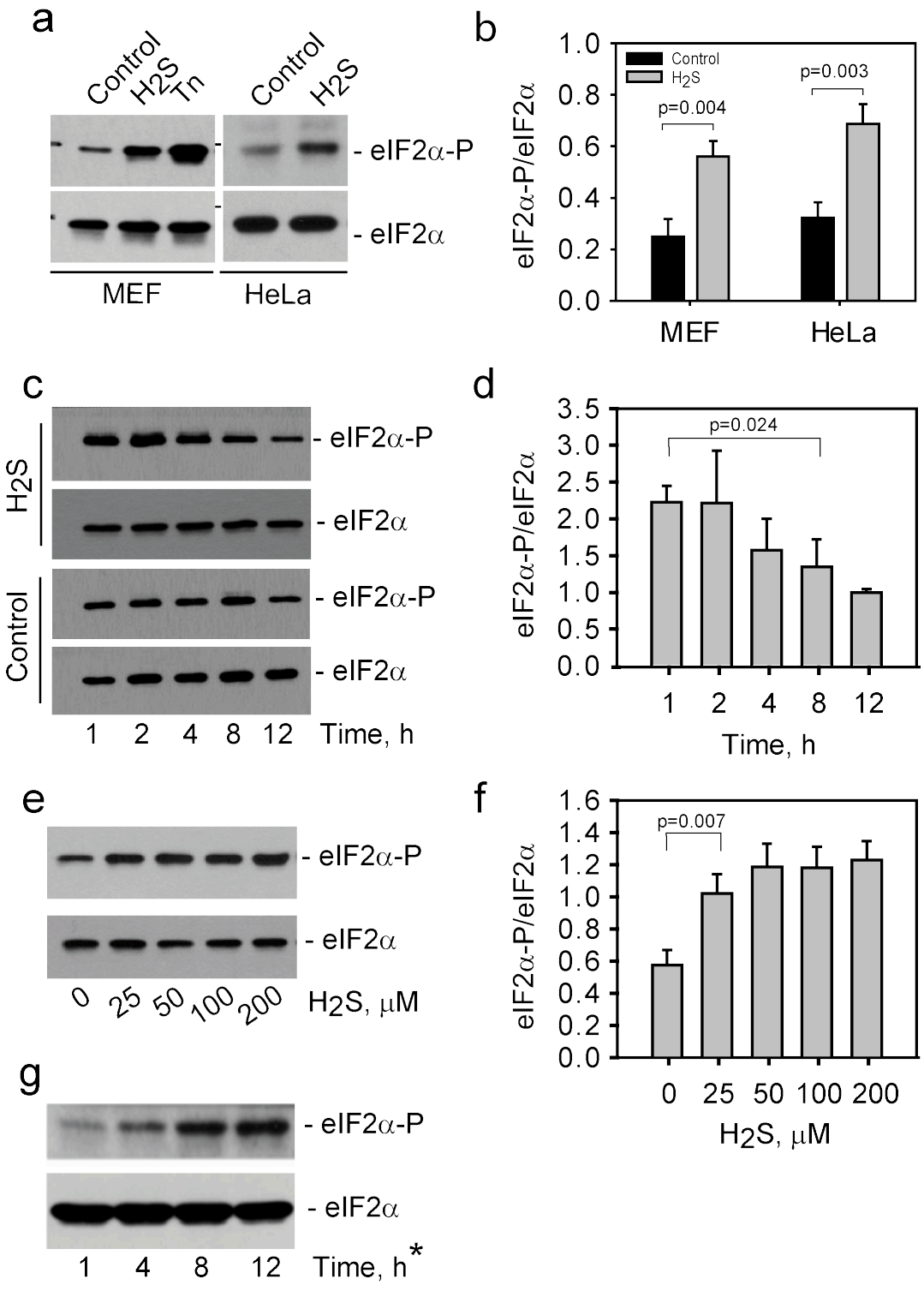

Figure 1. H_2S increases phosphorylated eIF2α level. a, Phosphorylation of eIF2α increases in cells treated with 100 μM NaHS. MEF cells and HeLa cells at a confluency of 80% were treated with NaHS for 2 h prior to western blotting analysis. MEF cells treated with ER stress inducing agent, tunicamycin, (0.5 μM) for 4 h were used as a positive control for eIF2α phosphorylation levels. Cells were washed twice with cold PBS on ice and lysed in RIPA buffer supplemented with complete protease inhibitor cocktail, 50 μg total protein was loaded per lane. **b**, Signal intensity was quantified for eIF2α-P and eIF2α from replicate western blotting experiments and expressed as eIF2α-P/eIF2α ratio. **c**, Time-dependent effect of H_2S on eIF2α-P levels after a single dose of 100 μM NaHS treatment. Cells grown in the absence of NaHS were processed for each time point as controls. **d**, Quantification of eIF2α-P signal from replicate western blotting experiments. **e**, Changes in eIF2α-P levels in response to increasing concentrations of H_2S. Cells were treated with the indicated concentrations of NaHS for 1 h prior to sample preparation. **f**, Quantification of eIF2α-P signal from replicate western blotting experiments. **g**, Increase in eIF2α-P level in response to repeated exposure to NaHS. Cells were supplemented with H_2S every 4 h and were harvested at 12 h after the first H_2S addition. Error bars represent ± SD, n=3. Signal for eIF2α, which represent total eIF2α, serves as an equal loading control. Error bars represent ± SD, n=3.

Figure 2.

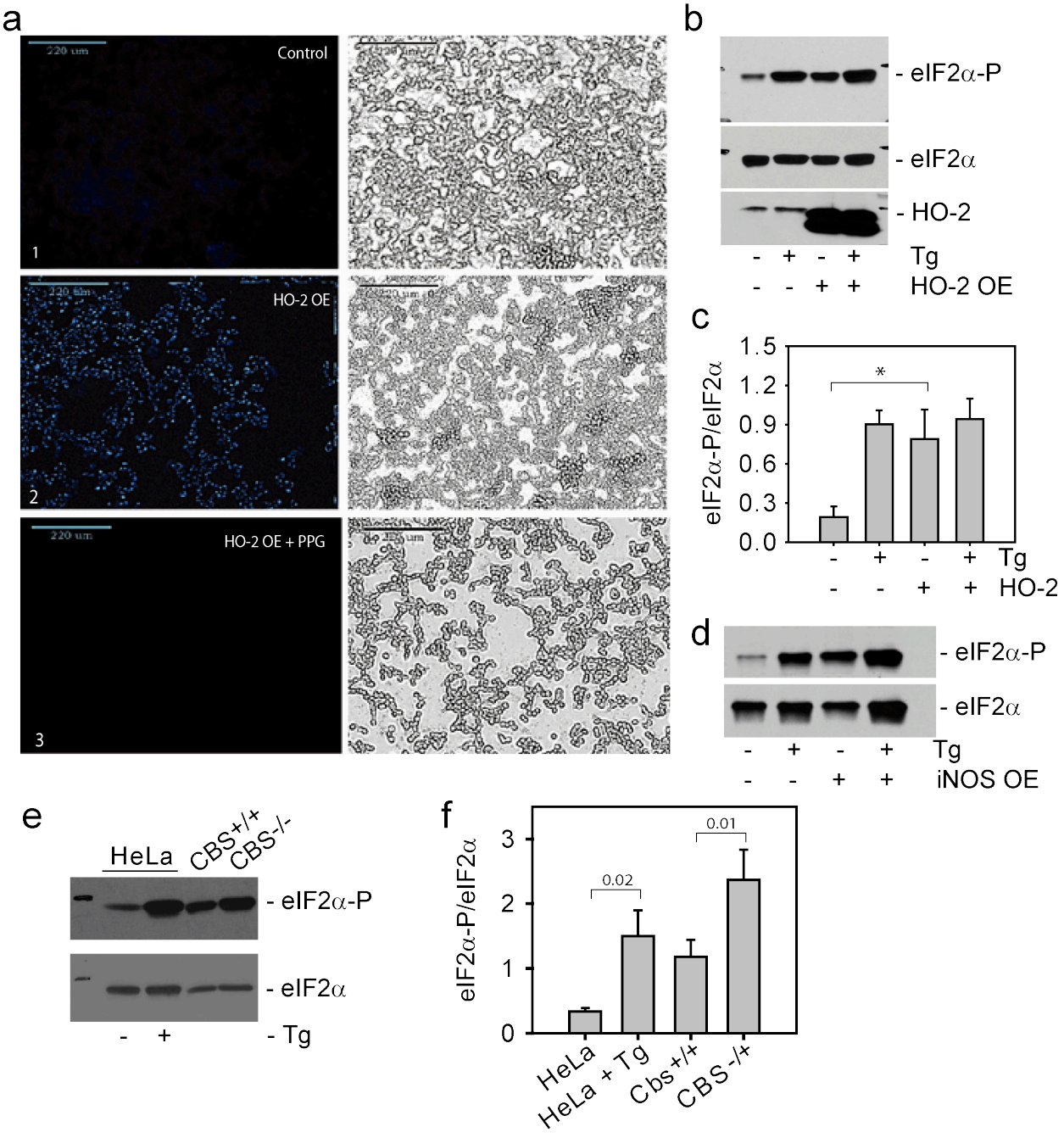

Figure 2. Induction of endogenous H_2S synthesis increases eIF2α-P levels. a, Visualization of endogenous H_2S using 7-azido-4-methylcoumarin in HEK293 cells. Panel-1 shows basal H_2S levels in control cells transfected with an empty plasmid, panel-2 shows increased H_2S levels in cells overexpressing HO-2 and panel-3 shows decreased H_2S levels in HO-2 overexpressing cells treated with propargylglycine (PPG) to inhibit the H_2S producing enzyme, CSE. The scale bars represent 200 μm **b**, Western blot analysis for eIF2α-P in HEK293 cells overexpressing HO-2 and in control cells transfected with an empty plasmid in the presence and absence of ER stress inducing agent, thapsigargin. **c,** Signals for eIF2α-P and eIF2α were quantified from replicate western blotting experiments. **d**, Western blot analysis for eIF2α-P in HEK293 cells overexpressing iNOS. **e**, Western bot analysis for eIF2α-P in liver tissue homogenates from wild type and $CBS^{-/-}$ mice. A total 50μg protein was loaded in each line. Extracts from HeLa cells +/- thapsigargin, 0.4 μM, were used as control. **f**, Signals for eIF2α-P and eIF2α were quantified from three replicate experiments and expressed as eIF2α-P/eIF2α ratio.

Figure 3.

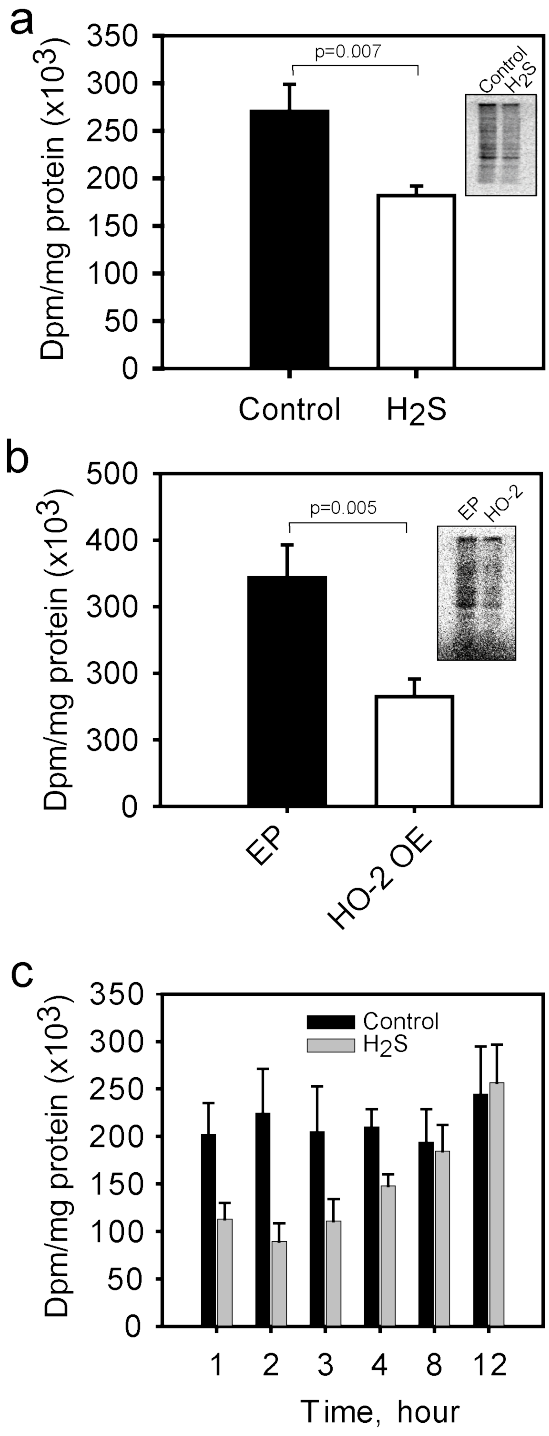

Figure 3. H_2S induced inhibition of protein synthesis. a, Rate of protein synthesis in MEF cells was measured by [^{35}S]-Met incorporation into proteins for 2 h in the presence and absence of NaHS (100 μM). The results represent the mean from three independent replicates. *Inset* is a representative aotoradiogram of proteins separated on 10% SDS-PAGE gel from H_2S treated and control cells. **b**, Protein synthesis rate were determined in HEK293 cells overexpressing HO-2 along with control cells transfected with an empty plasmid (EP) in the absence of exogenously added H_2S. *Inset* is a representative autoradiogram of proteins separated on a 10% SDS-PAGE gel from HO-2 overexpressing and control cells. **c**, Time-dependent behavior of protein synthesis rate in MEF cells after a single dose of NaHS (100 μM) treatment. NaHS was added to cells at 0 h and cells were continued to incubate for the indicated times. [^{35}S]-Met was added to the media 1 h before prior to sample preparation for each time point.

Figure 4.

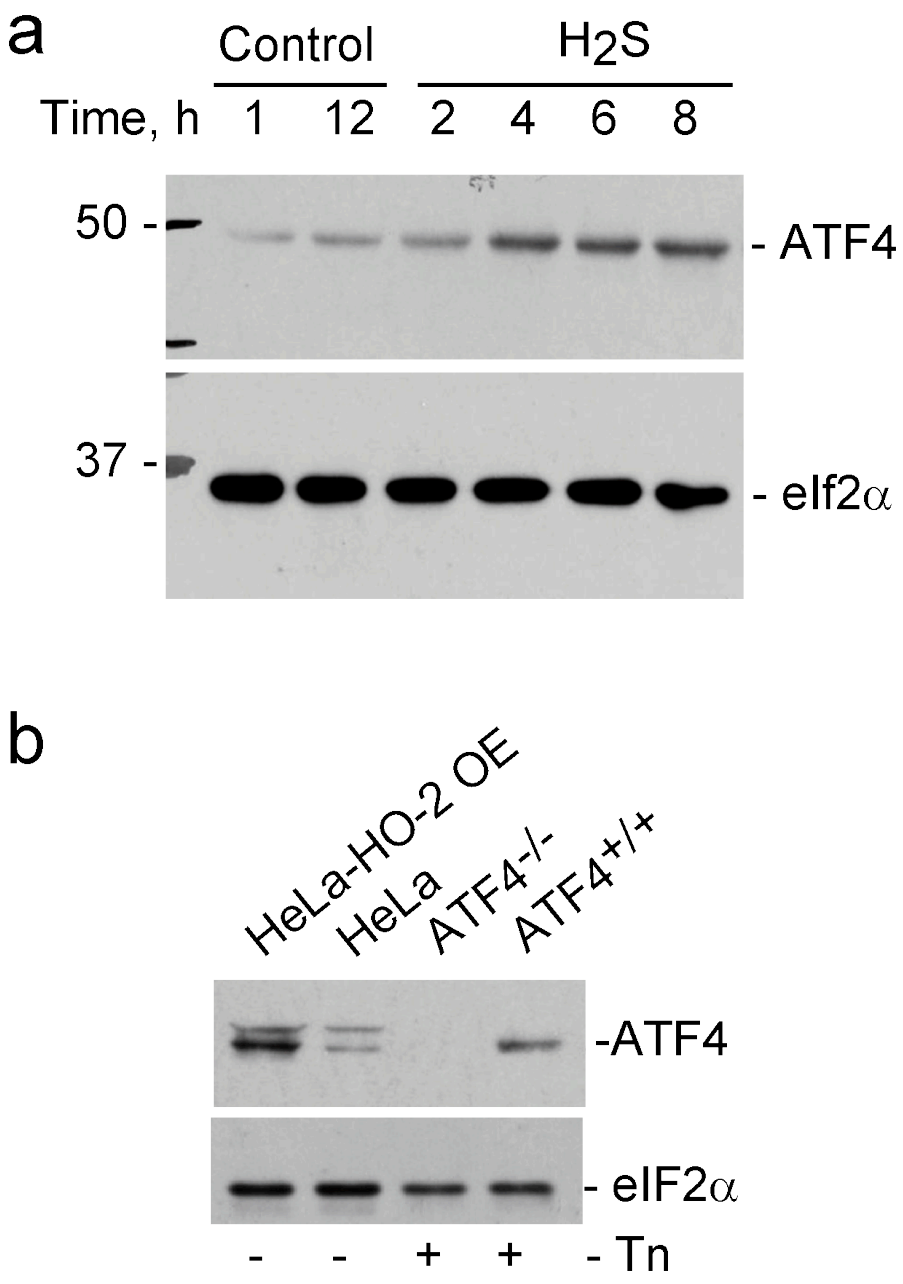

Figure 4. H_2S induces expression of ATF4. a, Western blot analysis of ATF4 protein in MEF cells treated with a 100 μM NaSH for the indicated times. Total protein (100 μg) was loaded in each lane. **b**, Analysis of ATF4 expression in HeLa cells stably expressing HO-2. Total protein (100 μg) was loaded in each lane. Extracts from $ATF4^{-/-}$ and $ATF4^{+/+}$ cells treated with tunicamycin were used as controls. eIF2α was used as equal loading control.

Figure 5.

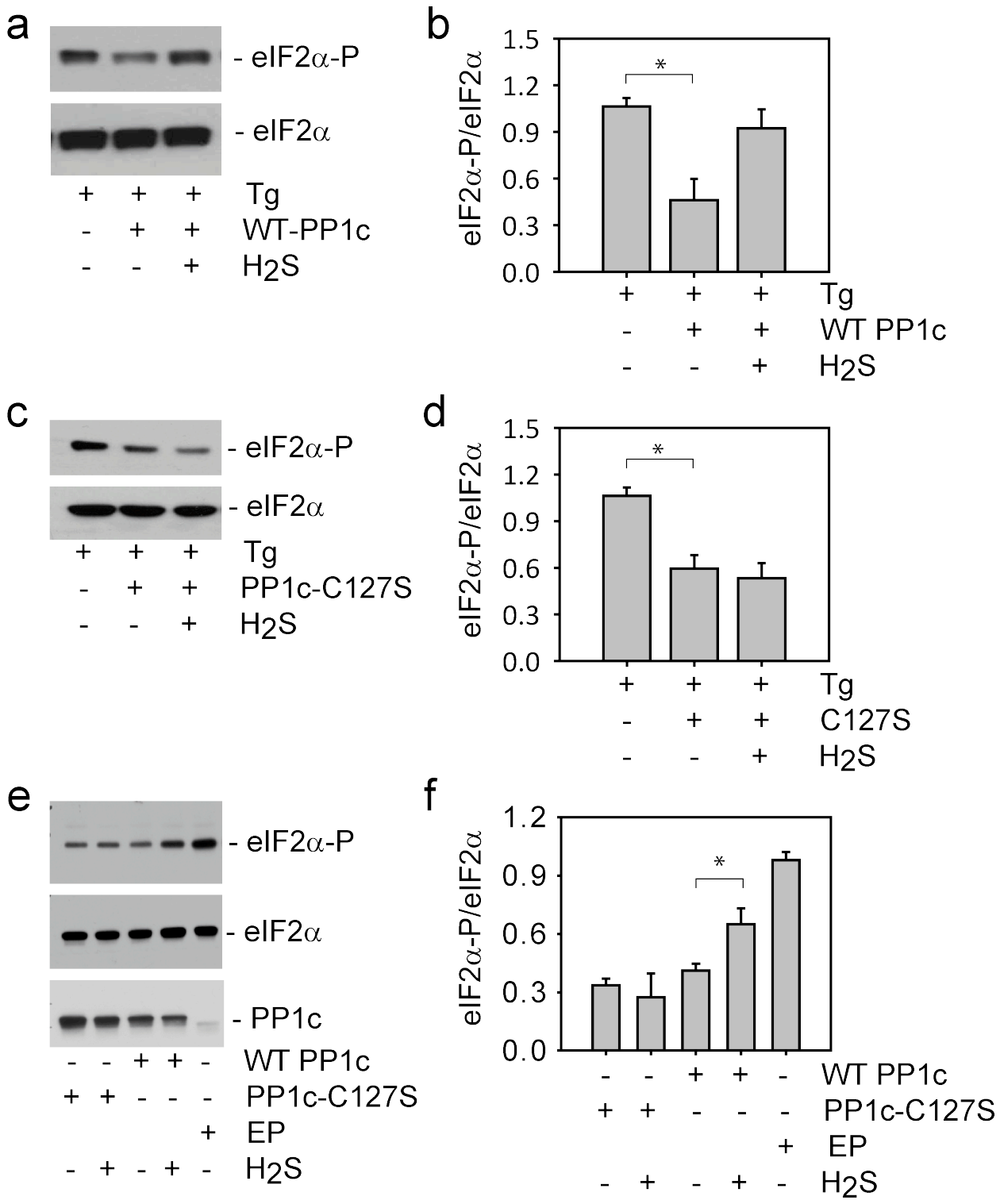

Figure 5. H_2S induced inhibition of PP1c activity. a, H_2S inhibits eIF2α dephosphorylation by PP1c. PP1c activity to dephosphorylate eIF2α were determined in reactions containing extracts (50-100 ug total protein) from Tg-treated HEK293 cells with or without NaHS pretreatment. Reactions were separated on a 10 %SDS gel and eIF2α-P and eIF2α levels were monitored by Western blot analysis. **b,** Quantified eIF2α-P and eIF2α signals presented as the ratio of eIF2α-P to eIF2α. **c**, Loss of the H_2S effect on the activity of PP1c-C127S. **d**, Signals for eIF2α-P and eIF2α in Western blots from replica assays were quantified. **e**, H_2S effect on eIF2α-P levels in cells overexpressing WT-PP1c and C127S-PP1c compared to control cells transfected with an empty plasmid. Thirty to forty eight h after transfection, cells were treated with 200 μM H_2S and continued to grow for 2 h prior to sample preparation. **f**, Quantified eIF2α-P signals from samples prepared from HEK293 cells expressing wild type or C127S mutant PP1c in the presence or absence of NaHS. EP donates empty plasmid. TR denotes transfection. Error bars represent SD. Asterisks (*) represent $p<0.05$.

Figure 6.

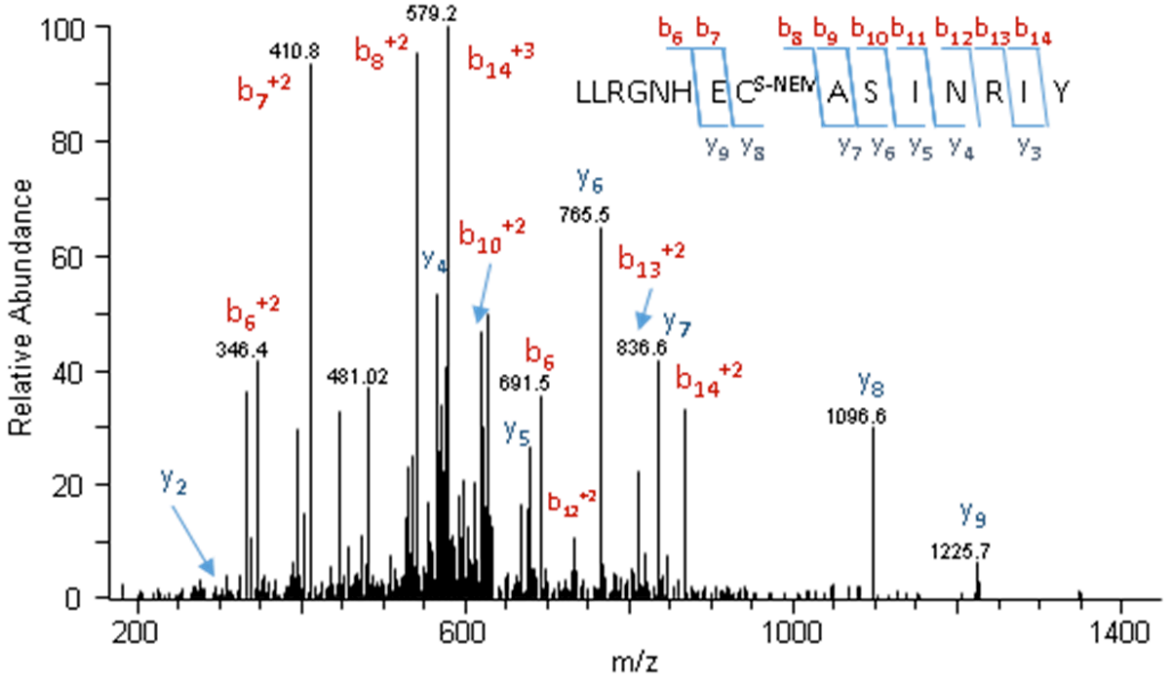

Figure 6. LC-MS/MS analysis of H_2S-modified PP1c. PP1c protein was incubated with NaHS at 25 °C and 20 µg of the treated protein was digested with trypsin and chymotrypsin. The resulting peptides were analyzed by LC-MS/MS. A single S-NEM modified PP1c peptide with a mass increase of 157.0192 (compared to unmodified peptide, mass increase: 125.1253) was identified and corresponds to Cys127 in the PP1c sequence. The MS/MS spectrum of the Cys127 chymotryptic peptide (LLRGNHECS-NEMASINRIY) is shown. This peptide was identified as the triply charged species; 639.313 Da, and has a mass error of -1.6 ppm. The MS/MS spectra contain several sequence specific ions including the b7 and b8 ions whose mass difference is consistent with S-NEM modification at Cys127.

Figure 7.

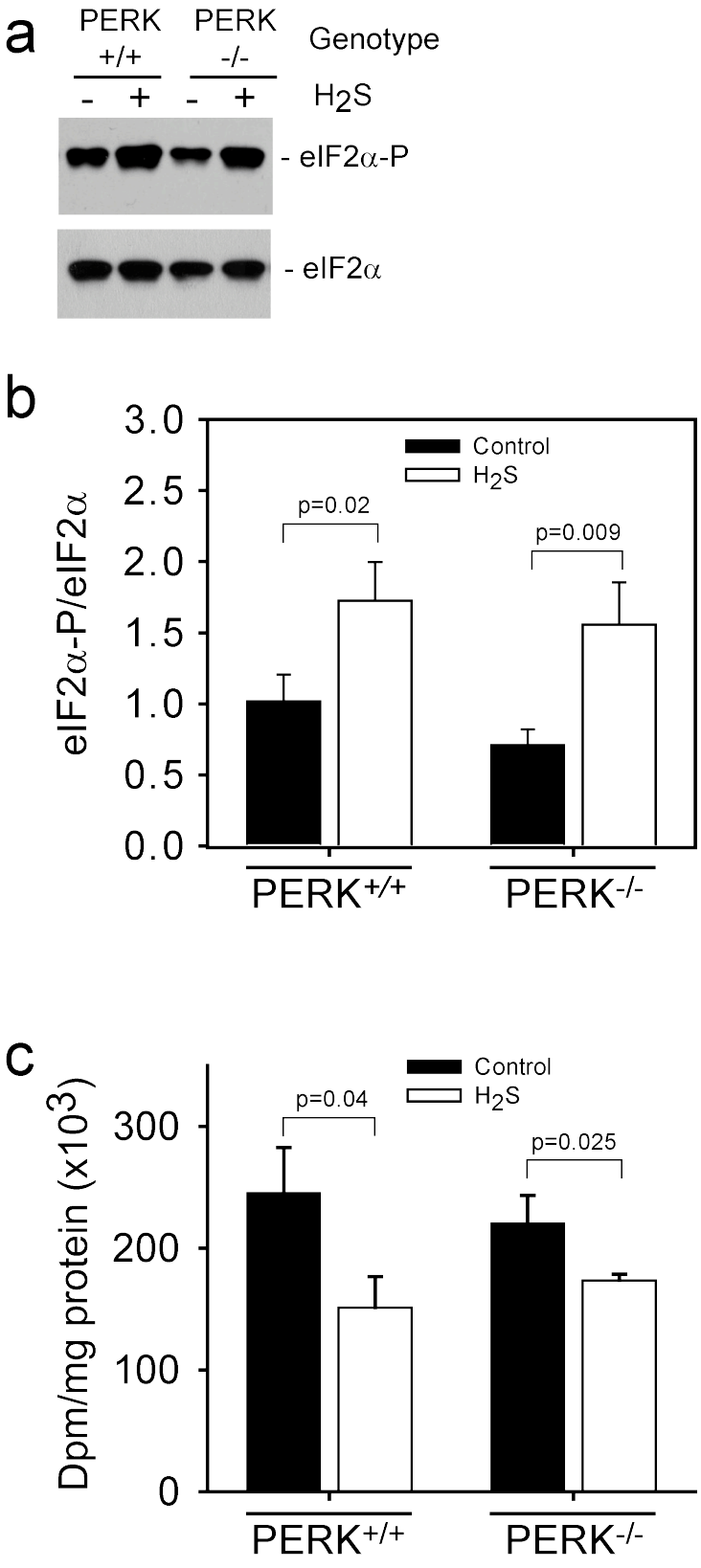

Figure 7. Perk kinase activation is not involved in H_2S-induced increase in eIF2α phosphorylation. a, Western blot analysis for eIF2α-P level in extracts from $Perk^{-/-}$ MEF cells along with wild type control cells with and without NaHS treatment, 100 μM for 1 h. **b**, Quantification of signal intensities for eIF2α-P and eIF2α from three independent experiments. **c**, Rate of protein synthesis in $Perk^{-/-}$ MEF cells along with wild type controls were determined by radiolabel incorporation from [^{35}S]-Met in the presence or absence of 100 μM NaHS. Error bars represent S.D. from three independent experiments.

Figure 8.

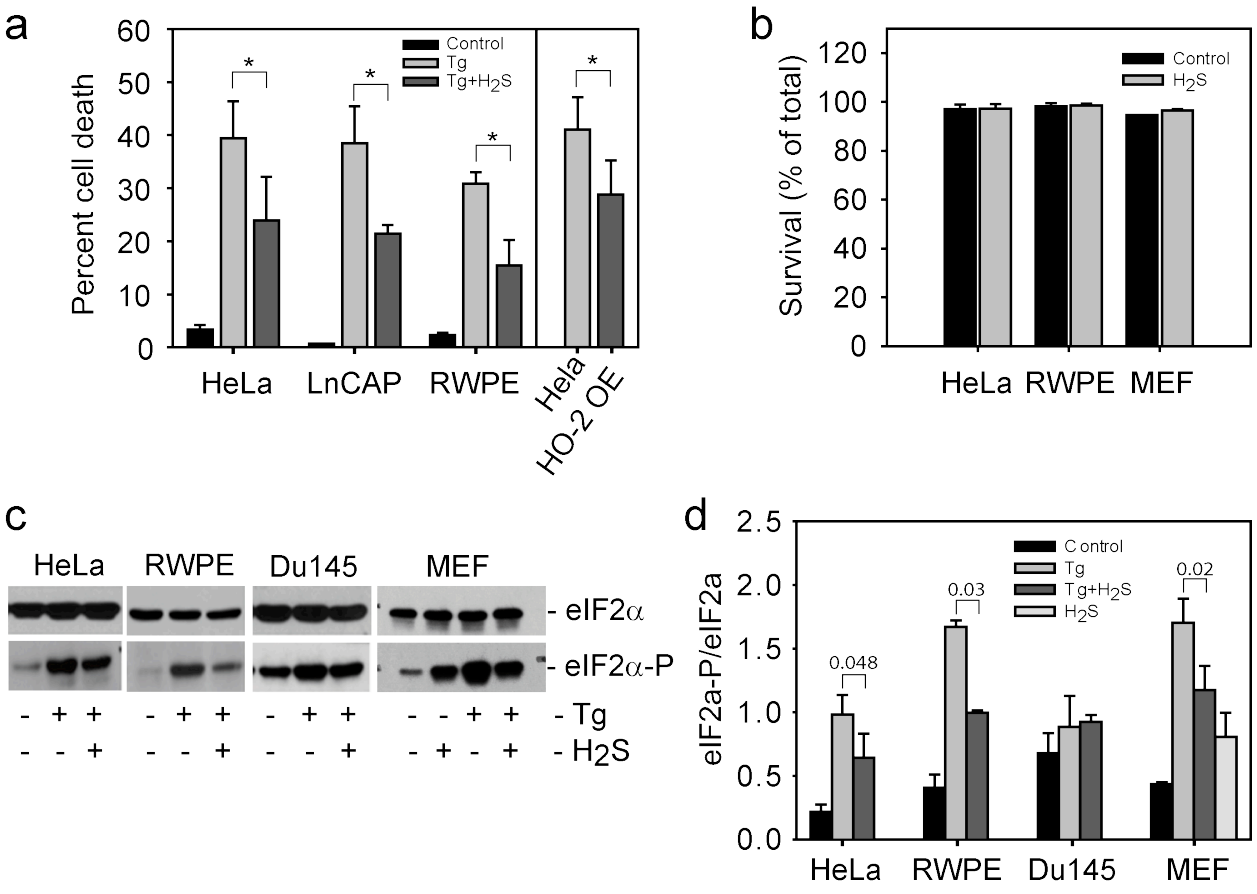

Figure 8. H_2S treatment and HO-2 overexpression increases resistance to ER stress. a, Cell viability was assessed for HeLa, RWPE and LNCAP cells in response to ER stress induced by 0.4 mM thapsigargin (8h) with and without NaHS pretreatment (200 μM final) for 2 h before the induction of ER stress. Percent cell death was calculated using the total cell number (dead and alive). Viability of HeLa cells stably overexpressing HO-2 and control cells was determined without NaHS treatment. Data represent mean ± SD, n=3. **b**, NaHS does not affect cell viability at 200 μM concentration. Cells were grown to a 60-70% confluency and NaHS was added to a final concentration of 200 μM. Cell viability were determined after 20-24 h using trypan blue to stain dead cells, which were counted using a microscope (with HeLa and RWPE cells) or analyzed by flow cytometry using propidium iodide to stain dead cells (for MEF cells). **c**, Western blot analysis for eIF2α-P levels in cells with ER stress induced by thapsigargin, 0.4 μM, with and without NaHS pretreatment. **d**, Quantification of signals from three independent experiments. Error bars represent SD, n=3-4.

Hydrogen sulfide modulates eukaryotic translation initiation factor 2α (eIF2α) phosphorylation status in the integrated stress response pathway

Vinita Yadav, Xing-Huang Gao, Belinda Willard, Maria Hatzoglou, Ruma Banerjee and Omer Kabil

J. Biol. Chem. published online June 21, 2017
